International Journal of Innovative Research in Advanced Engineering (IJIRAE) ISSN: 2349-2163
Issue 1, Volume 11 (November 2014) www.ijirae.com

Sodium nonstoichiometry effects on the crystal structure, electronic, optical and thermoelectric properties of sodium cobaltite

Mst. Taslima Akter
Department of Physics,
University of Rajshahi,
6205 Bangladesh

Md. Abdul Gafur
BCSIR,
Dhanmondi, Dhaka-1205
Bangladesh 6205

Md. Abdur Razzaque Sarker*
Department of Physics
Universityof Rajshahi
Bangladesh

The sodium-cobalt oxide Na_xCoO_2 is a promising candidate for thermoelectric applications since it may possess simultaneously large thermoelectric power and low resistivity. Electrical resistivity (ρ) and thermoelectric power (S) of Na_xCoO_2 samples were measured at various Na contents (x). A highly precise control of Na nonstiochiometry was attained by optimizing the synthesis procedure. With decreasing x, the value of ρ monotonically decreased, while the value of S increased. For x = 0.5, S reached a value as high as 124 μV/K at room temperature. Na nostoichiometry effects on the structural, electronic and optical properties of Na_xCoO_2 were investigated by first principle calculations.

Keywords— Calcination, Characterization, Density-functional theory, Solid-State reaction, Thermoelectric materials.

I. INTRODUCTION

Thermoelectric materials can directly convert heat into electric energy through thermoelectric power. They play a significant role in both waste heat recovery and active cooling applications. The thermoelectric device is environmentally friendly because it essentially produces no waste matter. Therefore, thermoelectric materials are studied worldwide for the reuse of exhaust heat from power plants [1]. Metal oxide materials are thought to be good candidate of thermoelectric materials because of their high thermal and chemical stabilities in air, easy manufacturing process, low cost and non-toxicity. Transition metal oxides AMO_2 (A: Alkali, M: Metal) with layered structure have been widely studied. Among them $NaCoO_2$ is extensively investigated as a promising candidate for a thermoelectric material.

The thermoelectric material is a material that shows large thermopower (*S*), low resistivity (ρ) and low thermal conductivity (κ) [2]. Terasaki *et. al.* discovered Na_xCoO_2 is a new thermoelectric oxide material with large thermoelectric power and low resistivity at room temperature, which makes this material suitable for future thermoelectric applications [3]. J.T. Hertz *et al.* reported that Na_xCoO_2 system exhibits remarkable electronic properties such as anomalously high thermopower [3,4], superconductivity when intercalated with water [5], and an unexpected metal-insulator transition [6]. The origin of large thermopower in this material remains an open question. Moreover, Na_xCoO_2 has been widely studied as solid-state cathode in Na batteries [7]. These observations have motivated investigation into the relationships between structure and properties in phases based on Na_xCoO_2.

D. J. Singh reported that the layered Co oxide, Na_xCoO_2, has remarkable transport properties [3] that are responsible for the high thermoelectric performance [8]. T. Motohashi *et al.* suggested that the spin state of cobalt ions plays a crucially important role in enhancing the thermoelectric power [9]. A very recent report of Y. Wang *et al.* showed that electron spins may play an important role in facilitating the high thermopower in Na_xCoO_2 [10]. Motohashi *et al.* reported that the carrier concentration has been found to be much higher in this compound than in some known thermoelectric materials such as Bi_2Te_3 and PbTe [11-14]. Their result of heat capacity measurements revealed that the effective mass of the carrier of this compound was as large as those of strongly correlated electrons. This was suspected to play an important role in the enhancement of thermoelectric power. M. Mikami *et al.* demonstrated that a strong electron-electron correlation plays an important role in producing the peculiar electronic properties of this compound [15]. However, very little research has been carried out on phases Na_xCoO_2, particularly on a single crystal. These observations have stimulated much experimental and theoretical work on Na_xCoO_2.

The thermoelectric, electronic and optical properties of Na_xCoO_2 might be governed by nonstoichiometry of sodium. Delmas *et al.* reported that the nostoichiometric Na_xCoO_2 compounds were metallic, while stoichiometric $NaCoO_2$ was a semiconductor [16]. In order to study the relationship between the sodium nonstoichiometry and thermoelectric properties, Na_xCoO_2 samples with precisely controlled sodium are indispensable. Recently, we established an unconventional sample-synthesis method that enables us to precisely control the Na content in Na_xCoO_2 samples. In this article, we discuss the effects of sodium nonstoichiometry on the thermoelectric, electronic, optical and transport properties of Na_xCoO_2. We also carefully studied the relationship between the chemical composition and physical properties of Na_xCoO_2. We characterized the thermoelectric behavior in the high temperature regime to evaluate the utility of such materials for power generation based applications. To clarify the physical and chemical properties, we studied the precise chemical bonding nature.

II. EXPERIMENT

Initially we studied the phase formation employing a thermobalance (TG/DTA 630) in order to establish the procedure for synthesizing Na_xCoO_2. A powder mixture of Na_2CO_3 and Co_3O_4 with molar ratio of Na:Co = 1.1:1 *i.e* x = 1.1, was heated in flowing O_2 gas with a heating program as shown in the inset of Fig.1. A representative thermogravimetric (TG) curve obtained for the raw material mixture is shown in Fig.1. From this TG analysis, it was found that the weight loss between 500 and 700 °C is too large (~ 7.5 %) due to decarbonation of raw materials (~6.0 %). This suggest that at temperature lower than ~ 600 °C, the chemical reaction between the raw materials may not be active yet and the observed weight loss is due to Na evaporation. There is no weight change above 750 °C where the phase formation is completed.

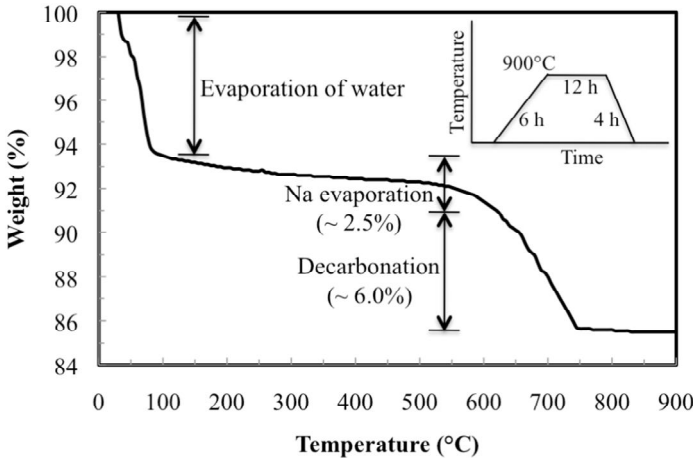

Fig. 1 Thermogravimetric curve for the phase formation process of $NaCoO_2$.The inset represents the heating program employed.

Based on the findings of the TG analysis on the phase formation, we employed a 'rapid heat-up technique to fire the raw materials to obtain Na_xCoO_2 samples with precisely controlled Na contents by avoiding Na evaporation prescribed by Motohashi *et al.* [11]. Before starting the synthesis, the reactants were dried in air in a oven at 100 °C for approximately 12 hours. After perfectly dried, Na_2CO_3 and Co_3O_4 were thoroughly mixed in a molar ratio Na/Co = 1.0, 0.75 and 0.5, using a hand mortar for 2-3 hours. A 10 % molar excess of Na_2CO_3 was added to compensate loss due to Na evaporation at high temperature.

The mentioned 'rapid heat-up' technique took place in three heating treatments. In first one, the mixed powder was hand pressed in an alumina crucible and directly placed in a furnace preheated at 750 °C to reduce the Na evaporation to the minimum extent. The temperature of the furnace was subsequently raised at 3 °C/min up to 800 °C. These target temperature was kept for 12 hours. Then, a similar second heat treatment was carried out at target temperature of 850 °C for 12 hours. Before the second heat treatment, the powder was reground to ensure homogeneity. After second heat treatment, the powder was grounded and pelletized in a 12 mm diameter using pressure gauze at 60 KN. For sintering, the pellets were placed in the furnace preheated at 700 °C and the temperature was raised at 3 °C/min up to 900 °C. The temperature was kept for 12 hours.

The powder samples were evaluated by X-ray diffraction using a CuK_α (λ=0.154 nm) radiation source in a BRUKER D 8-Discover X-ray diffractometer at room temperature. The diffraction angles (2θ) range between 10° and 90° was scanned. Fourier transform infrared (FTIR) spectrophotometer (Spectrum 100, Perkin Elmer) was used for FTIR transmission spectrum of the powder samples. Fine polishing was done for the disc like samples. The Agilent Precision Impedance Analyzer (Agilent technologies, Model: 4294A Japan) was used for measurements of frequency dependences conductance, impedance, dielectric constant and capacitance. The samples were characterized by UV–Visible spectrophotometer (Shimazu: UV–1650 PC) for wavelength dependence absorption spectrum. Resistivity measurements were carried out by the conventional four-probe method. Thermoelectric power (TEP) measurements were carried out by dc differential technique over a temperature range of 25 – 450 K, using a home made set up. Temperature gradient of ~1 K was maintained throughout the TEP measurements.

III. COMPUTATIONAL METHODS

The simulation calculations presented in this work were carried out by employing Cambridge Serial Total Energy Package (CASTEP) code [17] which utilizes the plane-wave pseudopotential based on the framework of density functional theory (DFT) method. The electronic exchange-correlation energy is treated under the generalized gradient approximation (GGA) in the scheme of Perdew-Brike-Ernzerhof [18]. The interactions between the ions and electron are represented by ultrasoft Vanderbilt-type pseudopotentials for Na, Co and O atoms [19]. The basis set of valence electronic states was set to be $2p^6 3s^1$ for Na, $3p^6 3d^7 4s^2$ for Co, $2s^2 2p^4$ for O.

The calculations use a plane-wave cut-off energy 700 eV for all cases. For sampling of the Brillouin zone a Monkhorst-Pack grid [20] of 12×12×2 *k*-points were employed for all calculations. All the structures were relaxed by Broyden-Fletcher-Goldfarb-Shenno (BFGS) methods [21]. For the geometry optimization, the convergence tolerances were set as follows: 5×10^{-6} eV/atom for the total energy, 0.001 eV/Å for the maximum force on atoms, 0.02 GPa for the maximum stress, 5×10^{-4} Å for the maximum atomic displacement. The total energy is conversed to within 0.01 m Ry/unit cell during the self-consistency cycle.

IV. RESULTS AND DISCUSSIONS

A. Structural properties

Crystalline $NaCoO_2$ powder was obtained by conventional solid-state reaction in the rapid heat-up technique with a final firing at 850 °C. The room temperature X-ray diffraction (XRD) pattern of Na_xCoO_2 samples with x = 1.00, is shown in Fig.2 that confirm the single phase consistent with a trigonal unit cell. Almost complete crystallization of $NaCoO_2$ with hexagonal symmetry takes place at 850 °C. T. Motohashi *et al.* showed that all the samples (x = 0.5–1.0) are reasonably single phase crystallizing in the hexagonal crystal structure [11, 22-23].

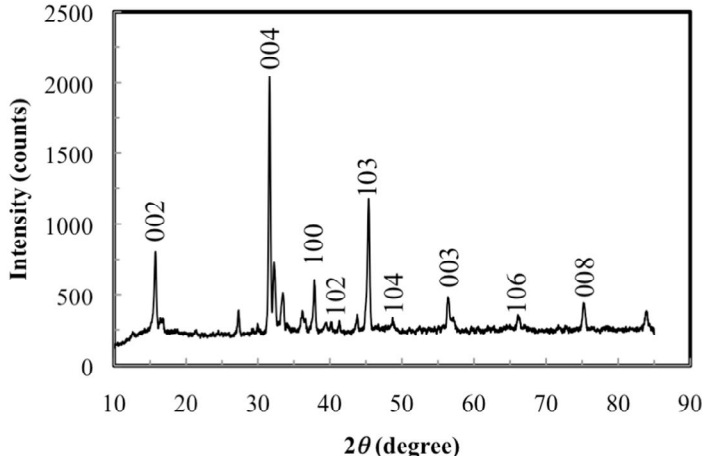

Fig. 2 X-ray diffraction pattern of the Na_xCoO_2 samples prepared by rapid heat-up technique.

Structural analyses were performed using computer program CASTEP code [17]. The BFGS algorithm is used to perform geometry optimization for hexagonal Na_xCoO_2 (x = 1) with trigonal unit cell at experimental lattice constant of $a = b$ = 2.889 Å and c = 15.609 Å [24]. The equilibrium lattice parameters and elastic constants are calculated at the optimized structure that contains the lattice constants of $a = b$ = 2.956 Å and c = 15.656 Å. The calculations were repeated for x = 0.75 and 0.5

TABLE I
THE CALCULSTED STRUCTURAL PARAMETERS OF NaxCoO2 (x = 0.5 – 1.0)

	$NaCoO_2$	$Na_{0.75}CoO_2$	$Na_{0.5}CoO_2$
Crystal structure	Trigonal	Hexagonal	Trigonal
Space group	166 (R3m)	194 ($P6_3/mmc$)	182 ($P6_3/22$)
Coordinates	Na (0, 0, 0) Co (0, 0, 0.5) O (0, 0, 0.2394)	Na_1 (0, 0, 0.25) Na_2 (0.33, 0.66, 0.75) Co (0, 0, 0) O (0.33, 0.66, 0.0915)	Na_1 (0, 0, 0.25) Na_2 (0.66, 0.33, 0.25) Co (0, 0, 0.5) O (0.33, 0.66, 2)
a (Å)	2.9560	3.4697	3.9363
c (Å)	15.6561	10.0713	9.4701
Unit cell volume $(Å)^3$	118.4764	105.0073	127.6767
E_0 (eV)	-9666.1622	-9044.1345	-9038.7281
B_0 (GPa)	174.3818	92.5871	51.6646
E_g (eV)	1.282	0.25	0.0

and it were shown that the structural parameters were affected by Na nonstoichiometry. The optimized structure parameters, *a*, *c*, *V*, the ground state energy E_0, the bulk modulus B_0, the band gap E_g of Na_xCoO_2 samples obtained with plane-wave pseudopotential DFT based CASTEP are given in Table (I). The crystal structure changes for reduction of x values. The values of ground state energy, E_0 increase by 622 eV for $Na_{0.75}CoO_2$ and by 628 eV for $Na_{0.5}CoO_2$. The calculated value of bulk modulus for $NaCoO_2$ is 174 GPa, for $Na_{0.75}CoO_2$ is 92 GPa and for $Na_{0.5}CoO_2$ is 51 GPa that is well agreement with experimental values. Therefore, the elastic properties of Na_xCoO_2 changes for reduction of *x* values.

In order to get physical insight of the chemical bonding structure and phase formation, we did the FTIR spectroscopic analysis that results are shown in the Fig.3. These results confirm the XRD observations showing that the vibration bands for precursors vanished and the vibration bands for the oxide network developed. The FTIR spectrum of Na_xCoO_2 powder has three characteristics bands at 523 cm^{-1}, 997 cm^{-1}, and 1384 cm^{-1} that ascribed to the vibration of metal oxygen band, indicating that $NaCoO_2$ was formed. Na – O was assigned to the presence of the absorption band at 523 cm^{-1} [25]. The strong absorption bands at 997 and 1384 cm^{-1} are assigned to Co – O stretching vibration and O – Co – O deformation modes of $NaCoO_2$, respectively. There are three sharp medium absorption peaks around 1638 cm^{-1}, which are all due to the vibrations of the sodium cobaltite crystal lattice. The results of FTIR analysis were good agreement with XRD results.

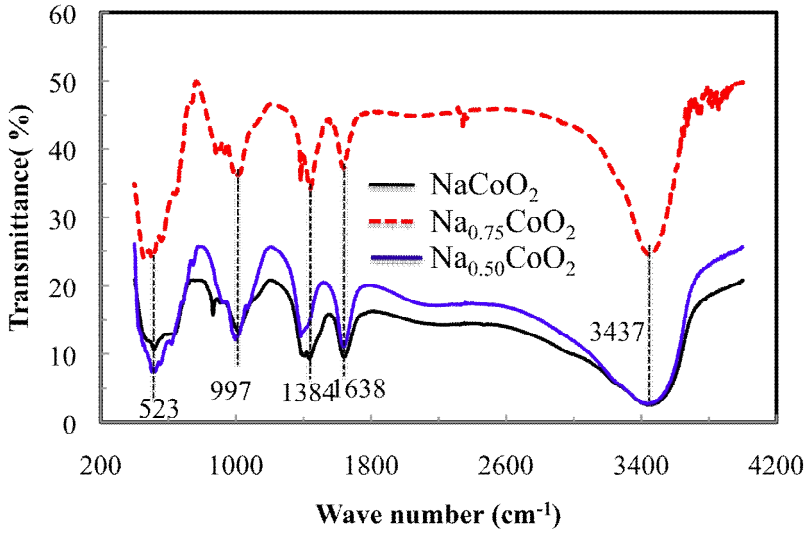

Fig. 3 FTIR spectrum of Na_xCoO_2 samples

B. Ellectronic properties

The spectrum of energy eigen values of a periodic system is band structure which determines the electronic and optical properties of the crystal. The electronic band structure of a solid describes ranges of energy that an electron is 'forbidden' of 'allowed' to have. The band gap is one of the most useful aspects of the band structure, as it strongly influences the electrical and optical properties of the material and stability of a compound toward oxidation or reduction. The band structure of Na_xCoO_2 was computed along the direction that contains the highest number of symmetry points within the Brillouin zone, namely, A-L-H-A-Γ-K-M-Γ. The calculated band structure of $NaCoO_2$, $Na_{0.75}CoO_2$ and $Na_{0.5}CoO_2$ are presented in Fig.4. Here, the top of the valence band is chosen to be the Fermi level (E_f = 0 eV). The valence band maximum and conduction band minimum occur at Γ point, making this material a direct band gap material (Γ–Γ). The calculated E_g values are given in Table (I). The calculated band gap of $NaCoO_2$, $Na_{0.75}CoO_2$ and $Na_{0.5}CoO_2$ are 1.28 eV, 0.25 eV and 0.0 eV. These results revealed that $NaCoO_2$ is a semiconductor and $Na_{0.75}CoO_2$ is metallic semiconductor however $Na_{0.5}CoO_2$ is a conductor. In the band structure of $Na_{0.5}CoO_2$, the valence band and conduction band are overlap in the Fermi level making it conductor.

In order to get more physical insight of the electronic band structure, we calculated the total density of states (TDOS) and partial density of states (PDOS) of $NaCoO_2$, $Na_{0.75}CoO_2$ and $Na_{0.5}CoO_2$. A comparison of TDOS is shown in Fig. 5(a). The TDOS is extended from about -7.0 eV to 10.0 eV where the Fermi-level position is set to 0 eV. Fig. 5(a) shows that TDOS of $Na_{0.75}CoO_2$ shifted slightly and that of $Na_{0.5}CoO_2$shifted effectively from TDOS of $NaCoO_2$. The density of states at the Fermi level is 8.71, 7.56 and 4.46 states/eV for $NaCoO_2$, $Na_{0.75}CoO_2$ and $Na_{0.5}CoO_2$, respectively. The DOS value at Fermi level reveals that stiochiometric $NaCoO_2$ is a semiconductor.

The partial contributions of *s*, *p* and *d* orbitals at E_F of Na, Co and O are displayed in Fig. 5(b–d). It shows that the valance band (VB) and conduction band (CB) are composed of Na 3*s*, Co 3*d* and O 2*p* orbitals. The lowest energy bands from -8 eV to -1.5 eV are derived mainly from the Co 3*d* states with little contribution from Na 3*s* states. The energy bands between -7 and 0 eV are dominated by hybridizing Na 2*p*, Co 4*d* and O 2*s*/2*p* states. Co 4*d* electrons are mainly contributing to the total DOS at the Fermi level and should be involved in the conduction properties.

It reveals that the transition between VB and CB is due to the O 2*p* and Co 3*d* states, because these states have maximum contribution in VB and CB. Co 4*s*/3*p* electrons do not contribute significantly at the Fermi level due to a scooping effect resulting from the presence of the Co 4*d* states. The value of total DOS at Fermi level is 8.74 states/eV. The atomic bonding characteristics are clearly illustrated in partial DOS. Na does not contribute significantly to the DOS at Fermi energy and therefore not involved in electronic transport. The highest contribution of partial DOS is for Co 4d states and its DOS value is 6 states/eV.

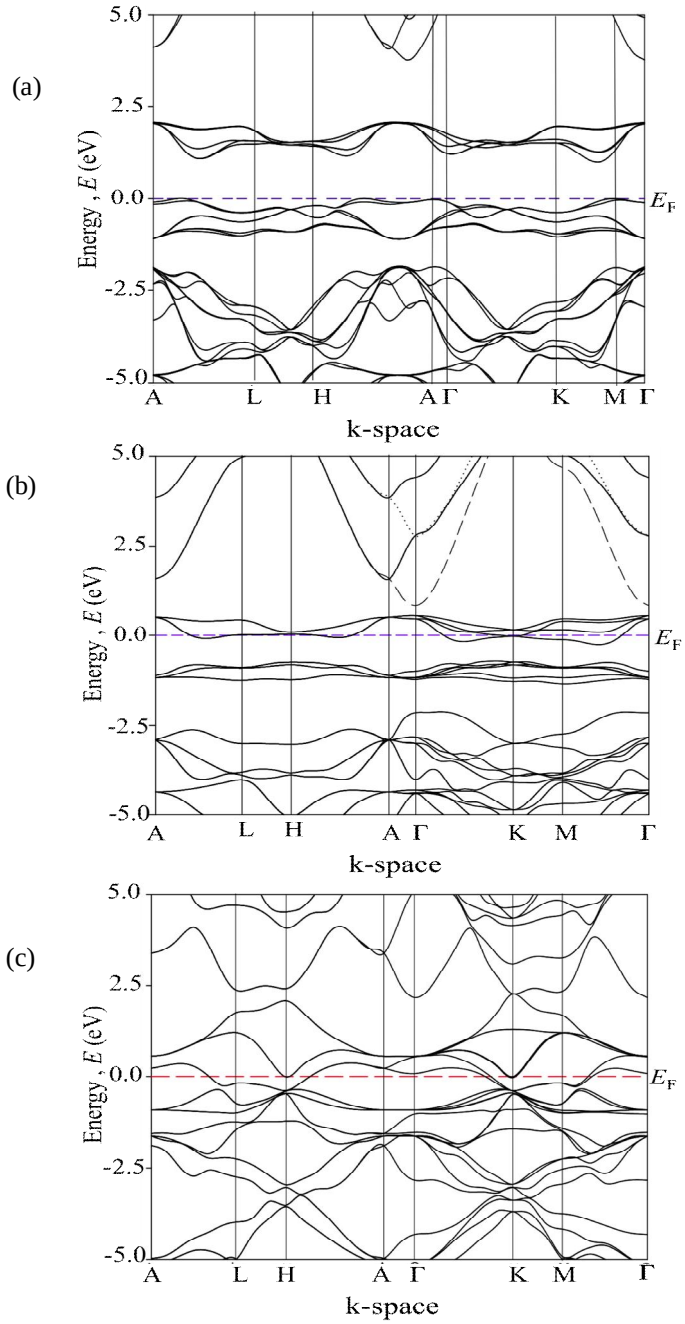

Fig. 4 Band structure of Na_xCoO_2 samples for (a) x = 1.0 (b) x = 0.75 and (c) x = 0.5

The temperature dependence ac conductivity of the samples was measured using four-probe technique from room temperature to 500 K. Fig.6 shows that the conductivity of the $NaCoO_2$ increase with temperature whereas that of $Na_{0.75}CoO_2$ and $Na_{0.5}CoO_2$ decrease. The dc conductivity strongly depends on the Na nonstoichiometry of Na_xCoO_2. The conductivity is very high in $Na_{0.5}CoO_2$ that reveals it a metallic conductor. The a-c conductance of the samples were measured by impedance analyzer, where the signal frequency was varied from 100 Hz to 10 M Hz and oscillating voltage 300 mV was applied.

Fig. 7(a) shows the frequency dependence a-c conductance of Na_xCoO_2 samples where the ac conductance increases with frequency. The frequency response ac conductance also depends on the Na nonstoichiometry of Na_xCoO_2 samples.

The ac conductance of $Na_{0.5}CoO_2$ is higher than that of $NaCoO_2$ and for $Na_{0.75}CoO_2$ is in between them. The impedance was also measured at frequency range 100 Hz to 10 MHz by impedance analyzer. Fig. 7(b) shows the frequency dependence impedance of Na_xCoO_2 samples. The impedance also depends on the Na nonstoichiometry of Na_xCoO_2 samples. The impedance of $Na_{0.5}CoO_2$ is higher than that of $NaCoO_2$ and for $Na_{0.75}CoO_2$ is in between them.

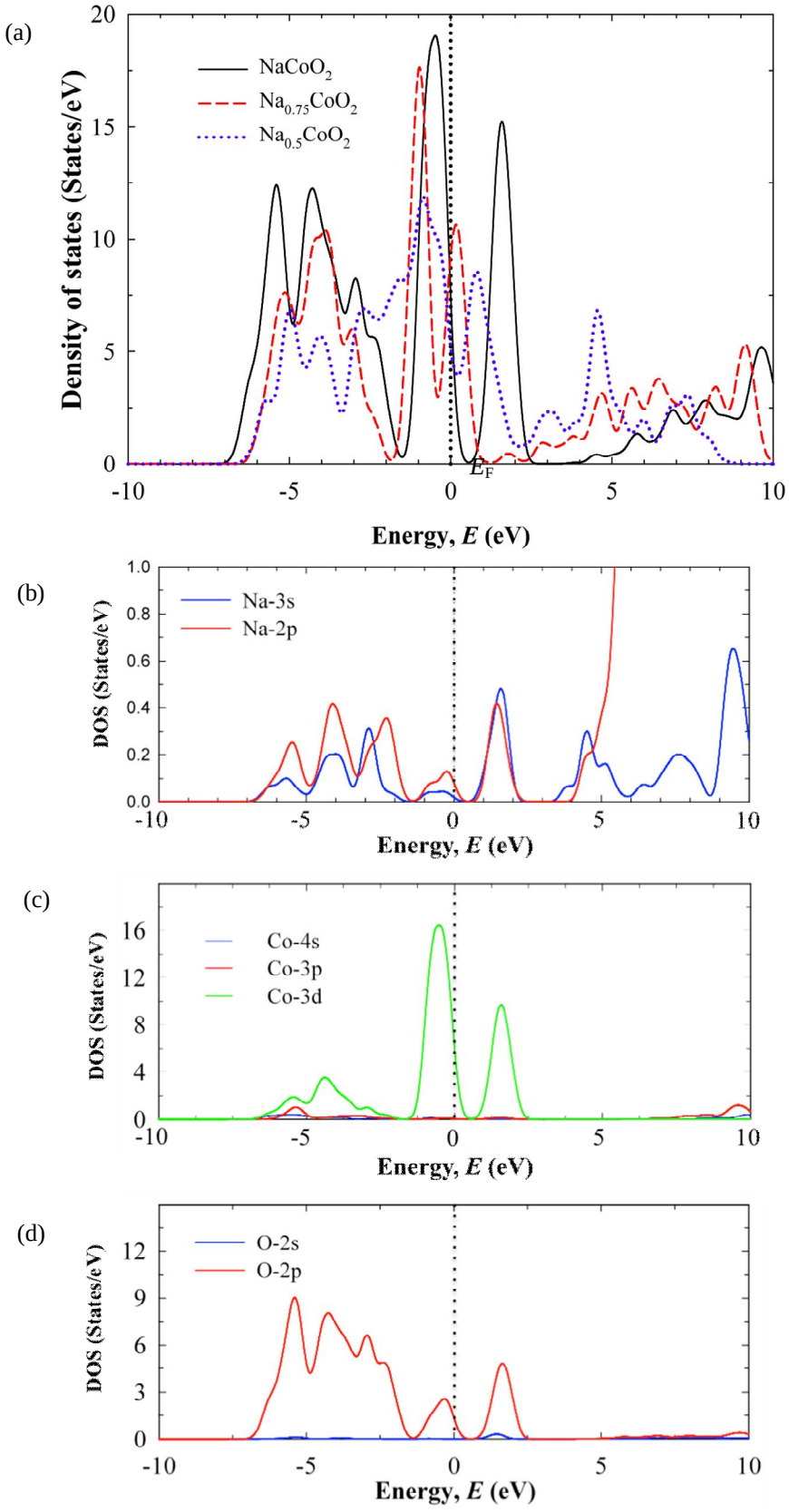

Fig. 5 (a) Total DOS of Na_xCoO_2 samples; Partial DOS of $NaCoO_2$ for (b) Na (c) Co and (d) O

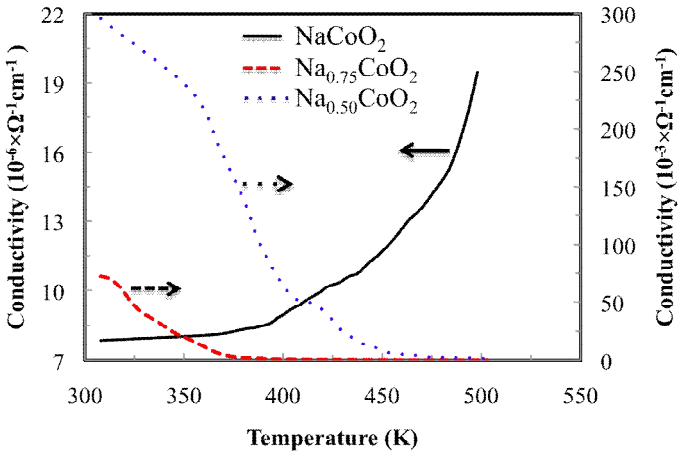

Fig. 6 Temperature dependence electrical conductivity of Na_xCoO_2 samples

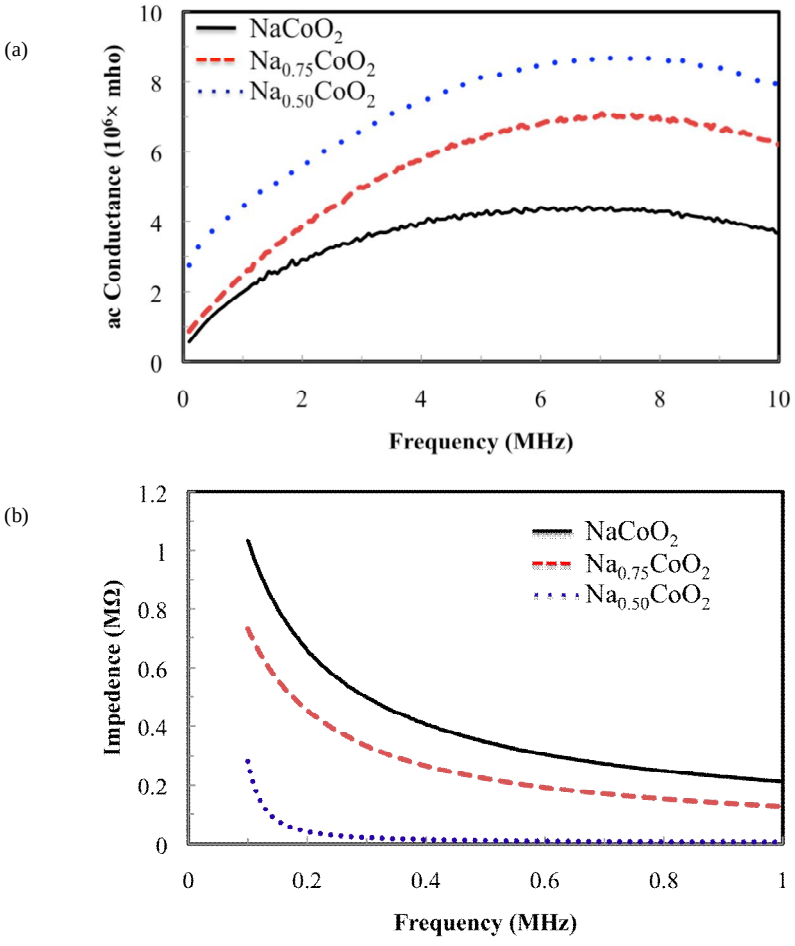

Fig. 7 The electrical frequency dependence of (a) electrical conductance and (b) impedance of Na_xCoO_2 samples

C. Optical properties

The analysis of the optical functions of solids helps to give a better understanding of the electronic structure. We calculate the optical functions of Na_xCoO_2 crystal for photon energies up to 25 eV for polarization vectors [100]. We have used a 0.5 eV Gaussian smearing for all calculations. This smears out the Fermi level, so that *k* points was more effective on the Fermi surface. The complex dielectric function is defined as, $\varepsilon(\omega) = \varepsilon_1(\omega) + i\varepsilon_2(\omega)$. The imaginary part $\varepsilon_2(\omega)$ is obtained from the momentum matrix elements between the occupied and the unoccupied electronic state. The real parts of the dielectric function are displayed in Fig. 8(a) for $NaCoO_2$, $Na_{0.75}CoO_2$ and $Na_{0.5}CoO_2$, respectively up to the photon energies of 15 eV. The peak of real part of the dielectric function is related the electron excitation.

Fig. 8(b) shows the reflectivity spectra as a function of photon energy for $NaCoO_2$, $Na_{0.75}CoO_2$ and $Na_{0.5}CoO_2$, respectively up to the photon energies of 25 eV. For polarization vector [100], it is found that the reflectivity in Na_xCoO_2 is high in visible and ultraviolet up to 15 eV region. The reflectivity reaches maximum at 11 eV for $NaCoO_2$, $Na_{0.75}CoO_2$ and at 15 eV for $Na_{0.5}CoO_2$. This results show that this material may use as promising coating material.

The refractive index as a function of photon energy for $NaCoO_2$, $Na_{0.75}CoO_2$ and $Na_{0.5}CoO_2$, respectively is shown in Fig. 8(c). The static refractive index at zero photon energy for $NaCoO_2$ is 3, for $Na_{0.5}CoO_2$ is 6 and for $Na_{0.75}CoO_2$ is 8. All the optical functions depend on the nonstoichiometry of Na in the Na_xCoO_2 samples. Dielectric properties of the Na_xCoO_2 samples were studied by precision impedance analyzer. Silver paste was coated on both surface of each sample before

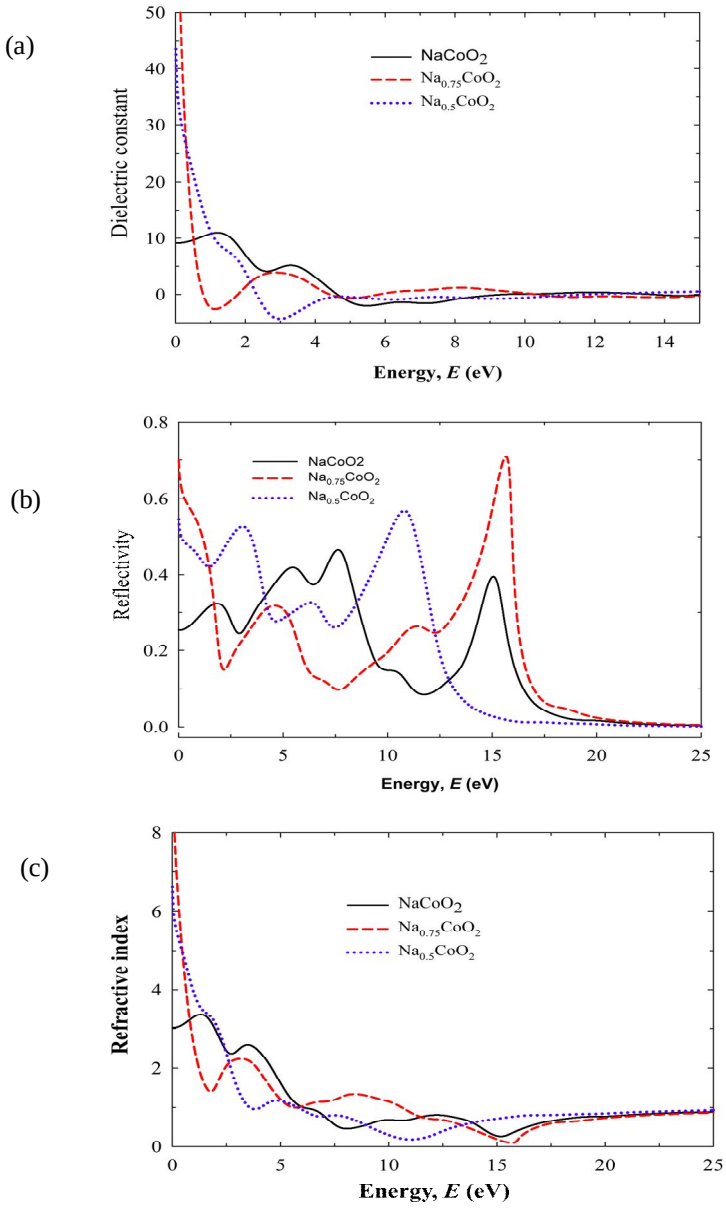

Fig. 8 (a) Dielectric function (b) reflectivity and (c) refractive index of Na_xCoO_2 samples as a functon of photon energy

measurement. Dielectric constant is a measure of materials ability to store electric charge. The frequency dependence capacitance of sample was measured within the frequency range 100 Hz to 10 MHz at room temperature as shown in Fig. 9(a). The capacitance of $NaCoO_2$ is high at low frequency region and decreases with increase of frequency for all samples. Fig. 9(b) shows the frequency dependence dielectric constant of Na_xCoO_2 samples. The capacitance of Na_xCoO_2 is high at low frequency region due to contribution of all kinds of polarization at low frequency, then decreases with increase of frequency and finally approaches to all most constant value above 6 MHz. This is due to the change of space charge, ionic and orientation polarization at higher frequencies [26]. Frequency response capacitance and dielectric constant strongly depends on the Na nonstoichiometry in the Na_xCoO_2 samples.

The UV-Visible absorption spectrum of the sample was recorded by using a UV-Vis spectrophotometer (Shimazu: UV–1650 PC) in the photon wavelength range between 200 – 800 nm.

Fig.10 show the absorption spectrum of Na_xCoO_2 samples. The absorption slightly decreases with increase of wavelength in the visible. There are some absorption peaks in the ultraviolet region for all the samples. There are two strong absorption peaks at 207 nm and 246 nm in the $NaCoO_2$ sample. There is a medium peak at 204 nm for $Na_{0.75}CoO_2$ and two very weak peaks at 209nm and 246 nm for $Na_{0.75}CoO_2$. These peaks reveal the absorption criteria of sodium cobaltite in the ultraviolet – visible region depending on the nonstoichiometry.

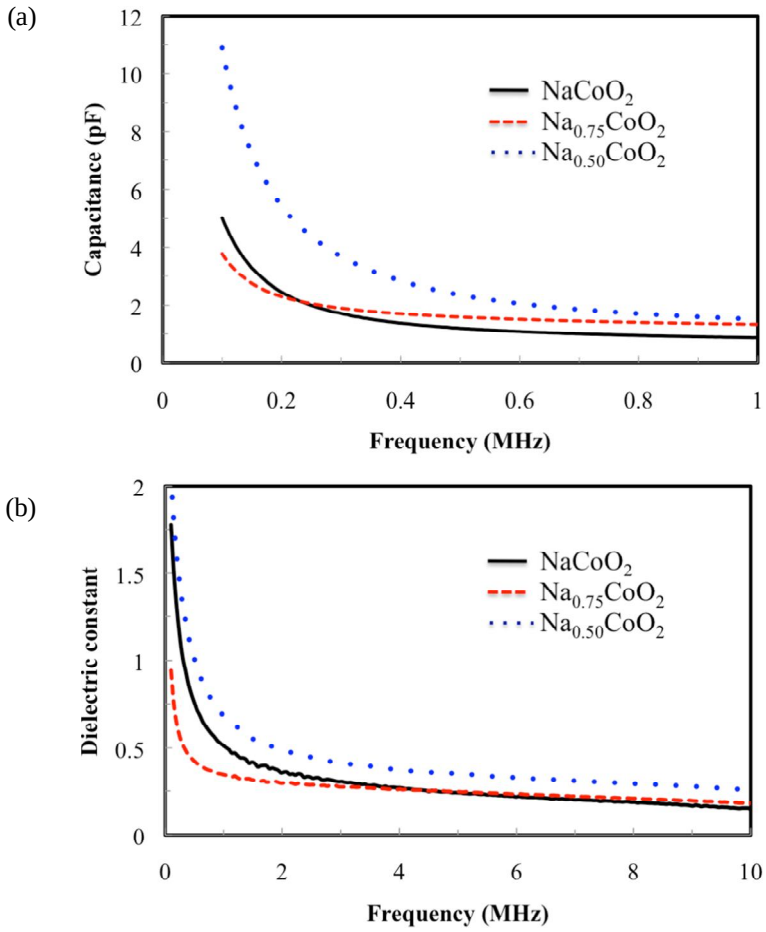

Fig. 9 The electrical frequency dependence of (a) capacitance and (b) dielectric constant of Na_xCoO_2 samples

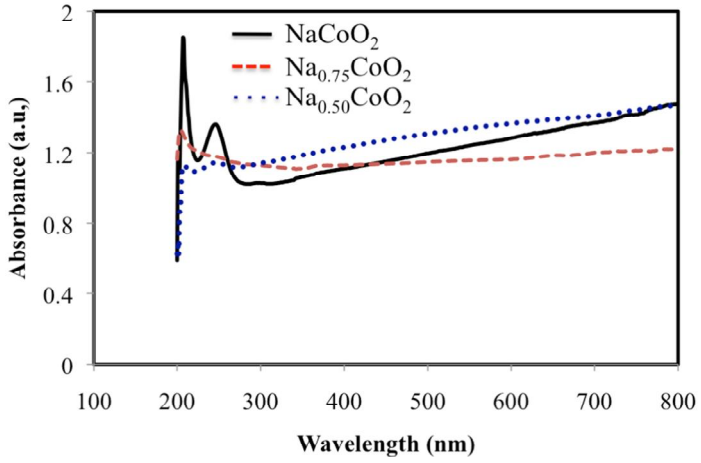

Fig. 10 The UV-Vis absorption spectrum of Na_xCoO_2 samples

D. Thermoelectric properties

Na_xCoO_2 oxide is one of the most promising thermoelectric oxides. The energy conversion efficiency of a thermoelectric device is mainly determined by the figure of merit (ZT) of its corresponding materials, which is expressed as $ZT = S^2T/\rho\kappa$, where S, ρ, k and T are Seebeck coefficient, electrical resistivity, thermal conductivity, and absolute temperature, respectively.

Therefore, good thermoelectric materials with a high *ZT* value should have a low electrical resistivity ρ, a high Seebeck coefficient *S*, and a low thermal conductivity κ. We measured the electrical resistivity, ρ of the Na_xCoO_2 samples with different Na contents (x=0.5–1.0) at room temperature to 500 K as shown in Fig. 11(a). The electrical resistivity of $NaCoO_2$ decreases with increasing temperature ($d\rho/dT < 0$) that shows the semiconducting behavior. On the other hand $Na_{0.5}CoO_2$ and $Na_{0.75}CoO_2$ show metallic behavior ($d\rho/dT > 0$) in the whole temperature range studied. We also calculated the thermal conductivity, κ using Wiedemann-Franz law from the measured resistivity for Na_xCoO_2 samples as shown in Fig. 11(b). Therefore, it represents the reverse nature of electrical resistivity.

The temperature dependence Seebeck coefficient, *S* of the Na_xCoO_2 samples is shown in the Fig.12. Very large values of Seebeck coefficients were obtained in spite of the relatively low electrical resistivity. This is considered to be caused by strong electron – electron correlations [14]. The Seebeck coefficient of all samples increase with increasing temperature and has a positive sign over the whole temperature range. The Seebeck coefficient strongly dependent on the Na nonstoichiometry in the Na_xCoO_2 samples. The room temperature Seebeck coefficient value for $NaCoO_2$, $Na_{0.75}CoO_2$ and $Na_{0.5}CoO_2$ are 92, 101 and 124 μV/K, respectively that are more than reported values [27].

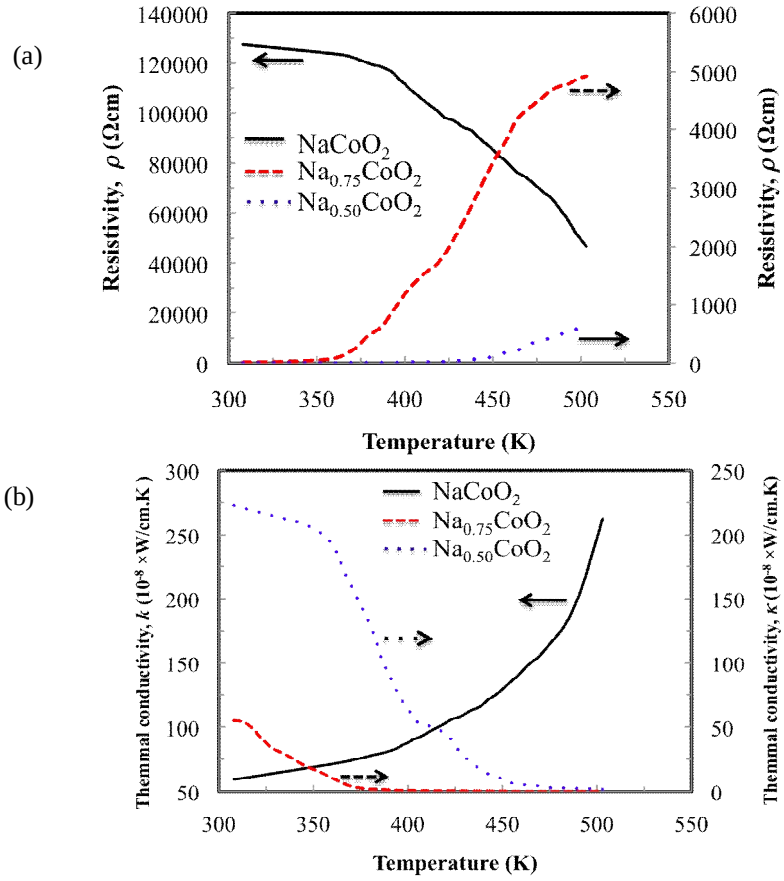

Fig. 11 The temperature dependence of (a) electrical resistivity, *r* and (b) thermal conductivity, *k* of Na_xoO_2 samples

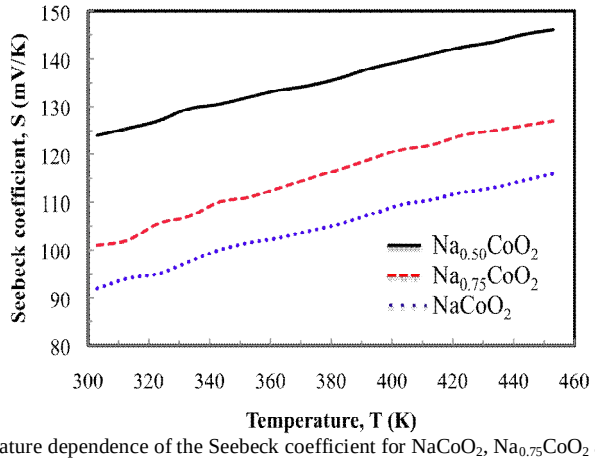

Fig. 12 Temperature dependence of the Seebeck coefficient for $NaCoO_2$, $Na_{0.75}CoO_2$ and $Na_{0.5}CoO_2$

V. CONCLUSIONS

Sodium cobaltite (Na_xCoO_2) single-phase powers have been successfully prepared by solid-state reaction using newly developed 'rapid heat-up technique'. This technique is most effective to control precisely the Na nonstoichiometry in the Na_xCoO_2 samples by avoiding unwanted Na evaporation during synthesis procedure. The phase formation condition was fixed by thermal analysis and single crystalline phase was confirmed by XRD study. With varying the Na concentration in the Na_xCoO_2 samples, structural, electronic and optical properties were reported experimentally and theoretically. The structural, electrical and optical measurements reveal that its all properties are well agreements with literature. The investigation of thermoelectric properties of the samples suggests that with decreasing Na content, the ρ value decreased and the S value increased simultaneously. By this report we want to propose that among Na_xCoO_2 (x=0.5–1.0) phases $Na_{0.5}CoO_2$ is the best thermoelectric materials with highest thermoelectric power.

ACKNOWLEDGMENT

This work was partially supported by the Rajshahi University Research Grant (No. A 774). Authors would like to thanks Rajshahi University, Rajshahi, Bangladesh authority for providing funds under the University Research Grant to carry out this work. The authors thank Mr. Md. Saiful Islam, Senior scientific officer, Cetral science laboratory, Rajshahi university for providing the experimental facilities.

REFERENCES

[1] K. Kurosaki, H. Muta, M. Uno, S. Yamanaka, Journal of Alloys and Compounds, vol. **315**, pp. 234–236, 2001.
[2] G. D. Mahan: Solid State Physics, vol. **51**, pp. 81-157, 1998.
[3] I. Terasaki, Y. Sasago, and K. Uchinokura, Phys. Rev. B, vol. **56**, pp. R12685- R12687, 1997.
[4] J. T. Hertz, Q. Huang, T. McQueen, T. Klimczuk, J.W.G. Bos, L. Viciu, and R.J. Cava, Phys. Rev. B, vol. **77** , pp. 075119-075131, 2008.
[5] K. Takada, H. Sakurai, E. Muromachi, F. Izumi, R.A. Dilanian, S. Sasaki, Nature, vol. **422**, pp.53-55, 2003.
[6] M. L. Foo, Y. Wang, S. Watauchi, H.W. Zandbergen, T. He, R.J. Cava, N.P. Ong, Phys. Rev. Lett. vol. **92**, pp. 247001.1-4, 2004.
[7] J. W. Fergus, *J. Eur. Ceram. Soc.*, vol. **32**, pp. 525-540, 2012.
[8] D. J. Singh, D. Kasinathan, Journal of Electronic materials, vol. **36**, pp. 736-739, 2007.
[9] T. Motohashi, M. Karppinen, and H. Yamauchi, Oxide Thermoelectrics, (Research Signpost, India) pp. 73-81, 2002.
[10] Y. Wang, N. S. Rogado, R. J. Cava, N. P. Ong, Nature, vol. **43**, pp. 425-428, 2003.
[11] T. Motohashi, N. Naujalis, R. Ueda, K. Isawa, M. Kappinen, Appl. Phys. Lett. vol. **79**, pp. 1480-1482, 2001.
[12] G. Mahan, B. Sales, J. Sharp, Phys. Today, vol. **50**, pp. 42-46, 1997.
[13] I. Terasaki, in *Proceedings of the 18th International Conference on Thermoelectrics*, Baltimore, MD, Aug. 29–Sept. 2, 1999.
[14] Y. Ando, N. Miyamoto, K. Segawa, T. Kawata, and I. Terasaki, Phys. Rev. B, vol. **60**, pp. 10580-10583, 1999.
[15] M. Mikami, M. Yoshimura, Y. Mori, T, Sasaki, R. Funahashi, M. Shikano, Jpn. J. Appl. Phys., vol. **42**, pp. 7383–7386, 2003.
[16] C. Delmas, J.J. Braconnier, C. Fouassier, P. Hagenmuller, Solid State Ionics, vol. **3/4**, pp. 165-169, 1981.
[17] S. J. Clark, M. D. Segal, M. J. Probert, C. J. Pickard, P. J. Hasnip, M. C. Payne, Z. Kristallor. vol. **220**, pp. 567-571, 2005.
[18] J. P. Perdew, K. Bruke, M. Ernzerhof, Phys. Rev. Lett. vol. **77**, pp. 3865-3868, 1996.
[19] D. Vanderbilt, Phys. Rev. B, vol. **41** , pp. 7892 – 7895, 1990.
[20] H. J. Monkhorst, J. D. Pack, Phys. Rev. B, vol. **13**, pp. 5188-5192, 1976.
[21] T. H. Fisher, J. Almolf, J. Phys. Chem., vol. **96**, pp. 768-772, 1992.
[22] T. Motohashi, R. Ueda, E. Naujalis, T. Tojo, I. Terasaki, T. Atake, M. Karppinen, and H. Yamauchi, Phys. Rev. B, vol. **67**, 0644061.1-5, 2003.
[23] J. Sugiyama, H. Itahara, J. H. Brewer, E. J. Ansaldo, T. Motohashi, M. Karppinen and H. Yamauchi, Phys. Rev. B, vol. **67**, pp. 214420.1-5, 2003.
[24] Y. Takahashi, Y. Gotoh, J. Akimotoa, Journal of Solid State Chemistry, vol. **172**, pp. 22–26, 2003.
[25] D. Berger, N. van Landschoat, C. Ionica, F. Papa, V. Fruth, J. Optoelectron. Adv. Mater., vol. **5**, pp. 719-723, 2003.
[26] W. D. Kingegy, *Introduction to Ceramic* (John Wilely & Sons, Inc. New York, 1967).
[27] D. J. Singh, Phys. Rev. B, vol. **61**, pp. 13397-13402, 2000.

